The Structure of the Protonated Adenine Dimer by Infrared Multiple Photon Dissociation Spectroscopy and Electronic Structure Calculations

Khadijeh Rajabi,[†] Kelly Theel,[‡] Elizabeth A. L. Gillis,[†] Gregory Beran,[‡] and Travis D. Fridgen*[,†]

Department of Chemistry, Memorial University of Newfoundland, St. John's, Newfoundland, Canada, A1B 3X7, and Department of Chemistry, University of California, Riverside, California 92521

Received: April 9, 2009; Revised Manuscript Received: May 29, 2009

The infrared multiple photon dissociation (IRMPD) spectrum of electrosprayed adenine proton-bound dimers were recorded in the gas-phase inside the cell of a Fourier transform ion cyclotron resonance spectrometer coupled to a tunable optical parametric oscillator/amplifier infrared laser. While gas-phase B3LYP/6-31+G(d,p) calculations indicate that the four lowest isomers are essentially isoenergetic, comparisons of the experimental and predicted IR spectra suggest that only two of the four isomers are observed in the experiment. However, computed solvation effects, as modeled using both a polarizable continuum model and microsolvation with five explicit water molecules, preferentially stabilize these two observed isomers, consistent with the interpretation of the IRMPD spectra. This work shows that for these small species the solvent-phase structure is preserved. It also demonstrates the potential danger of using gas-phase calculations to predict the structures of gaseous ions born in solution, such as those from an electrospray source.

1. Introduction

Adenine (6-aminopurine, $C_5H_5N_5$) plays a crucial role in biochemistry. For example, it is a main component of adenosine triphosphate (ATP), NAD^+, and nucleic acids to name a few. Nucleic acids have been used in constructing materials[1] such as nanomachines, nanoscaffolds, and DNA computers.[2] DNA bases themselves have gained interest as components of self-assembling structures. For example, 2-D sheetlike nanostructures containing doubly protonated adenine have self-assembled from low-pH aqueous solutions containing adenine, hydrogen halide, and iodide. These structures have been isolated and characterized by X-ray crystallography.[3]

Adenine itself has been the topic of numerous quantum mechanical molecular structure studies to explore geometries, proton affinities, protonation, polyhydration, tautomerism, the structure of the amino group in terms of planarity, and the mechanism of double proton transfer in adenine-containing complexes.[4−14] The presence of "rare" or noncanonical tautomeric forms of DNA bases is closely related to mispairing of purines and pyrimidines, causing spontaneous point mutations.[15−17] Therefore, there is an increasing interest to investigate the structure and tautomerism of the DNA bases. The N9H tautomer of adenine was calculated to be the most stable (Scheme 1) in the gas phase by some 30−35 kJ mol^{-1}.[18,19] Protonation of the N9H tautomer at N1 is found to be thermodynamically preferred in the gas phase.[20] Gu et al.[4] explored the water-assisted intramolecular proton transfer in the tautomers of adenine using density functional theory (DFT, B3LYP/6-311G(d,p)) calculations and found that the high-energy imino form of the tautomers of adenine are stabilized by about 8−12 kJ mol^{-1} in the presence of water due to enhancement of the conjugated π electron system found in the imino form of adenine. Because of its larger dipole moment, the N7H tautomer of adenine was found to be preferentially stabilized in the presence of water, where it lies only about 16 kJ mol^{-1} above the N9H tautomer.[4] A larger concentration of the N7H tautomer, then, would be expected in aqueous solutions and in biological systems than indicated by gas-phase calculations. A water molecule was also found to reduce the energy barrier to the tautomerization by acting as both a proton donor and acceptor, thereby assisting the proton transfer isomerization.[4] The tunneling effect in the intramolecular proton transfer in adenine was investigated using the parabolic barrier approximation and one-dimensional model.[21,22] The tunneling rates were calculated to be 10^{10} times larger than the classical one for the gas phase and 10^3-10^4 times larger for the water-assisted process. In addition, the assignment of the bands in the infrared spectra of argon- and nitrogen-matrix-isolated adenine and its ^{15}N isotopomers (substituted at N9 or N7 positions) indicated that only the N9H tautomer of adenine was identified.[23] The results of these studies represent the solid phase since the source of matrix-isolated adenine is from heating solid adenine in vacuum and entraining the vapor in matrix gas prior to being condensed on a cryogenic substrate.

SCHEME 1

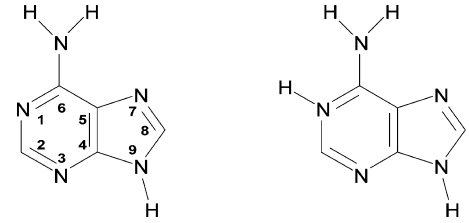

Proton-transfer reactions are important in biological systems since they can lead to mutations.[16] It is therefore important to investigate the changes in chemical properties of bases due to protonation. Many experimental and theoretical studies have been conducted on protonated nucleic acid bases and related compunds[24−29] due to the remarkable effect protonation has on conformational structure.[30] For example, base protonation has

* To whom correspondence should be addressed. E-mail: tfridgen@mun.ca.
[†] Memorial University of Newfoundland.
[‡] University of California, Riverside.

10.1021/jp9033062 CCC: $40.75
Published on Web 06/23/2009

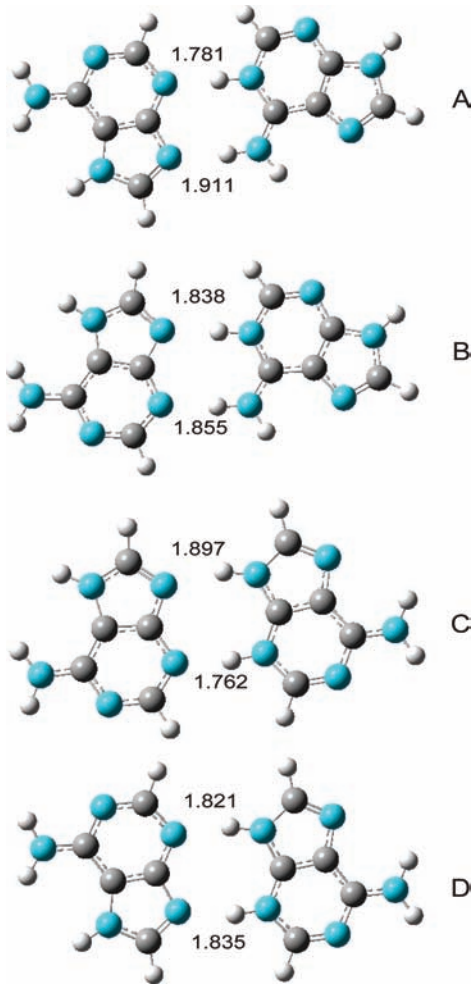

Figure 1. B3LYP/6-31+G(d,p) structures of the four lowest-energy proton-bound adenine dimers.

been implicated in the transformation of the B to Z structures of DNA.[31,32] Knowledge of the protonation site is also essential for the design of some drugs which regulate the activity of a selected gene by stabilizing the triple helix formed between the target base sequence and an oligonucleotide.[33] The triple helix structure inhibits transcription resulting in its therapeutic effect.[34] Russo et al.[25] have performed gradient-corrected density functional computations with triple-ζ-type basis sets to determine the preferred protonation site and the absolute gas-phase proton affinities of the most stable tautomers of the DNA bases and for the first time predicted the gas phase basicity order among four DNA nucleic acid bases to be

guanine > cytosine > adenine > thymine

A better redistribution of electron density was found in the most favorable protonated species. The nature of the highest-occupied molecular ortbial (HOMO), molecular electrostatic potential, and charge distribution together can explain the effects that stabilize the most stable protonated structures. Proton affinity values of 873.6 (T), 958.6 (C), 944.7 (A), and 963.6 (G) kJ mol^{-1} at 298 K were obtained, in a fair agreement with available experimental data.

The small energy differences between the adenine tautomers and among their conjugate acids make the identification of the most stable tautomers theoretically challenging. Relative tautomer stabilities are highly sensitive to changes in the treatment of electron−electron correlation and/or the one particle basis.[25,12] Therefore, experimental techniques that target alternative properties are potentially very useful. IR spectroscopy is obviously a powerful technique to study adenine cluster systems; however, other spectroscopic techniques (such as photoexcitation) have been widely used to elucidate changes in the electronic structure and dynamics of adenine due to the presence of a proton. For instance, Marian et al.[35] produced protonated adenine ions by electrospray, stored and cooled them in a Paul trap, and dissociated them using resonant photoexcitation with nanosecond UV laser pulses. By comparing their photofragmentation spectra with computed vertical excitation spectra, it was determined that protonation mainly occurs at the N1 position of an N9H tautomer of adenine, with a possible contribution from the N3 protonated N7H tautomer, which lies only 1.9 kJ mol^{-1} higher in energy.

Infrared multiple photon dissociation (IRMPD) spectroscopy[36−38] provides more direct evidence of cation structure. For instance, Atkins et al.[39] have used IRMPD spectroscopy in the N−H/O−H stretching region along with electronic structure calculations to determine that the lowest energy structure of sodium-bound glycine dimers consists of two symmetric bidentate ligands. Similarly, for the aliphatic amino acid proton-bound homodimers composed of glycine, alanine, and valine as well as the heterogeneous alanine/glycine mixture an ion-dipole complex in which the N-protonated amino acid is bound to the carbonyl oxygen of the second monomer was found to be the dominant structure.[39,40] In another recent study, the oxazalone structure was confirmed for the b_2^+ ion produced from collision-induced dissociation of the protonated AGG peptide while the protonated cyclic dipeptide is a diketopiperazene.[41] Much less work has been done on DNA bases and related compounds. Salpin et al.[42] identified the lowest energy structures of the protonated pyrimidic bases using IRMPD spectroscopy in the 900 to 2000 cm^{-1} region.[43] Lithium cationized complexes of thymine and uracil have also been studied in the gas phase by IRMPD spectroscopy in the N−H/O−H stretching region.[44] On the basis of a combination of experimental and theoretical data, it was found that the lithium cation in both thymine and uracil complexes most likely bind to O4 to form linear Li^+-bound dimers. Hydration of these Li^+-bound dimers resulted in significant structural changes to enable strong interbase hydrogen bonding, similar to that in the Watson−Crick model of DNA.

In recent theoretical work by Liu et al.,[9] nine stable proton-bound adenine dimers, $(C_5H_5N_5)_2H^+$, formed from the N9H tautomer of adenine and the N1 protonated N9H tautomer were found. In some of the proton-bound dimers, the proton partially or completely transferred from the protonated adenine to the neutral. While one might expect the proton-bound dimer to consist of the most stable neutral and protonated monomer forms, Hud and Morton[45] demonstrated that the four proton-bound dimers composed of the N9H tautomer protonated at N1 and the N7H tautomer of adenine are by far the lowest energy proton-bound dimers and that the four isomers have fairly similar binding energies. In the present work the structure of the adenine proton-bound dimer is explored by combination of theoretical and IRMPD techniques. By comparison of the experimental IRMPD spectra with theoretical predictions of the vibrational spectra for various isomers, we hypothesize that only one or two isomers are observed experimentally. While our predicted gas-phase thermochemistry data cannot explain this observation, we perform calculations that suggest that the experimentally observed isomers are thermodynamically favored in solution.

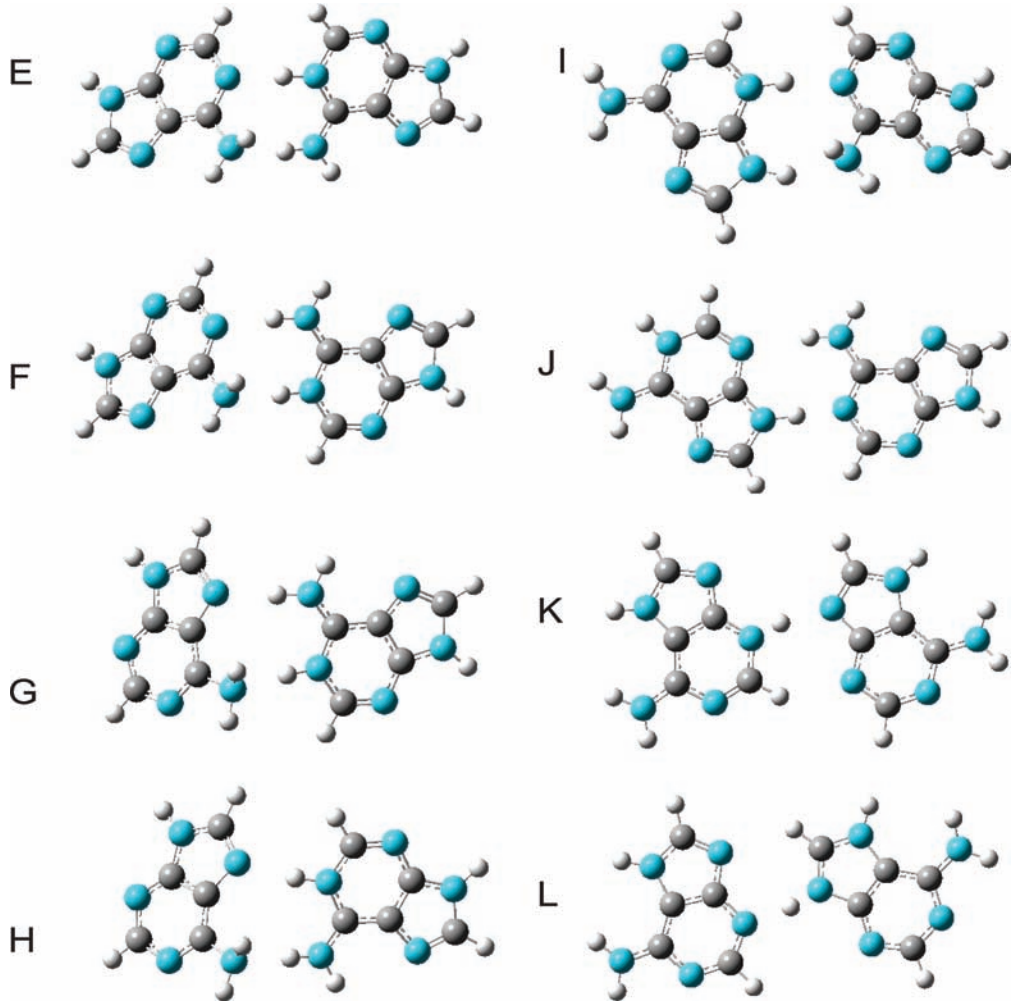

Figure 2. B3LYP/6-31+G(d,p) structures of eight high-energy proton-bound adenine dimers.

Therefore, we propose that only two of the most stable gas-phase dimers are prevalent in solution and that these solution-stable dimers are predominantly the ones that are electrosprayed and observed in these gas-phase experiments.

2. Methods

2.1. Experimental Section. The details of coupling the ApexQe Bruker Fourier transform ion cyclotron resonance (FT-ICR) mass spectrometer with a 25 Hz Nd:YAG pumped Laservision optical parametric oscillator/amplifier (OPO/OPA) laser have been presented previously.[46] Adenine proton-bound dimers were electrosprayed from ~5 mM solutions of adenine in 18 MΩ Millipore water which had been slightly acidified with a few drops of 1 mM HCl solution. Protonated adenine dimer (*m*/*z* 271) was isolated in the ICR cell by standard ejection techniques. Absorption of the infrared laser light resulted in dissociation of the proton-bound dimer, which was monitored by a change in mass of the parent ion. The IR laser scan rate was 0.5 cm^{-1} s^{-1} with irradiation times of 2.0 s. This corresponds to a step size of 1 cm^{-1} between points in the IRMPD spectra. IRMPD efficiency is defined as the negative of the natural logarithm of precursor ion intensity divided by the sum of the fragment and precursor ion intensities.

2.2. Computational Section. Optimized structures, dimer interaction energies, harmonic vibrational frequencies, and statistical thermodynamic quantities of the various proton-bound adenine dimer isomers were computed using the B3LYP density functional and the 6-31+G(d,p) basis set in the Gaussian 03 software package.[47] Single point MP2/6-311++G(2d,p) calculations were also done on the B3LYP/6-31+G(d,p) structures. Thermodynamic quantities employing the MP2 electronic energies and the B3LYP thermal corrections are reported as MP2/6-311++G(2d,p)//B3LYP/6-31+G(d,p) energies. In addition, we refine the predicted energies using the recently developed double-hybrid B2P3LYP density functional[48] with the cc-pVTZ basis.[49] Standard density functionals exhibit known deficiencies in treating van der Waals interactions,[50] and double-hybrid functionals[51] attempt to correct for this deficiency by mixing in Moller−Plesset (MP2)-like long-range correlation into the functional. The B2P3LYP functional significantly outperforms B3LYP for systems where noncovalent interactions are important, so we use it here. The cc-pVTZ basis is the recommended basis set for use with B2P3LYP, since the empirical parameters in the functional were fit using this basis. To compensate for basis set superposition errors (BSSE), the standard Counterpoise correction[52] was also considered. All B2P3LYP calculations were performed using a developmental version of Q-Chem, version 3.1.[53] Because analytical gradients of the B2P3LYP functional are currently unavailable, we utilize B3LYP/6-31+G(d,p) structures and harmonic frequencies (for computing thermodynamics).

Two additional approximations are invoked to accelerate the B2P3LYP energy calculations. First, just as in the original B2P3LYP paper, we use the resolution-of-the-identity (RI)

TABLE 1: Binding Energies (kJ mol^{-1}) of the Four Lowest-Energy Isomers of the Proton-Bound Adenine Dimer Relative to N9H Adenine and N1-Protonated-N9H Adenine (Experimental Value for ΔH(500 K) = 127 ± 4 kJ mol^{-1})

	B3LYP/6-31+G(d,p)		B2P3LYP/cc-pVTZ[a]	
isomer	ΔE_{elec}^{CP} [b]	ΔH(500 K)[c]	ΔE_{elec}^{CP} [b]	ΔH(500 K)[c]
A	113.8	106.8	132.4	125.4
B	111.3	104.1	129.5	122.3
C	111.0	104.7	131.1	124.8
D	109.4	102.9	129.5	123.1

[a] Using B3LYP/6-31+G(d,p)-optimized geometries. [b] Counterpoise-corrected electronic interaction energies. [c] Enthalpies computed using B3LYP/6-31+G(d,p) structures and frequencies.

TABLE 2: Computed Relative Enthalpies for Various Adenine Proton-Bound Dimer Structures

structure	B3LYP/6-31++G(d)//B3LYP/6-31G(d,p)[a,c]	B3LYP/6-311+G(d)[b]	MP2/6-311++G(2d,p)//B3LYP/6-31+G(d,p)[c]	B2P3LYP/cc-pVTZ//B3LYP/6-31+G(d,p)[c]
A	0		0.0 (0.0)	0.0 (0.0)
B	2.6		3.1 (1.9)	3.1 (1.9)
C	2.5		0.7 (1.3)	0.5 (1.1)
D	4		2.3 (2.4)	2.2 (2.3)
E	24.3	0	17.7 (21.1)	
F	27.8	3.8	23.1 (26.6)	
G	31.5	13.1	25.5 (30.0)	
H		15.1	24.5 (28.6)	
I		14.1	23.0 (26.1)	
J		15.9	36.2 (35.8)	
K			37.4 (34.5)	
L			46.2 (39.7)	

[a] Reference 45. [b] Reference 9 and relative to structure E. [c] 298 K enthalpies and (free energies in parentheses), relative to structure A.

approximation[54] and the auxiliary cc-pVTZ fitting basis[55] to speed the MP2 portion of the B2P3LYP calculation substantially. Second, we utilize a dual-basis Hartree−Fock (HF)/MP2 calculation.[56] In this approach, the HF/cc-pVTZ solution is approximated by taking the converged HF density matrix from a carefully chosen smaller basis set, projecting the density matrix into the larger cc-pVTZ basis and taking a single HF iteration in the larger basis. By use of these approximations, the energy of a 5-water-molecule-solvated adenine dimer structure (1044 basis functions in the cc-pVTZ basis) can be computed in about 6 h on a single processor on a modern workstation. At the same time, these two approximations introduce negligible additional errors into the relative energies.

Two separate strategies were used to address aqueous solvation effects on the proton-bound dimers. First, polarizable continuum model (PCM) calculations[57] at the B3LYP/6-31+G(d,p) level are performed to address bulk solvation effects. Adenine proton-bound dimer gas-phase structures were reoptimized and frequencies computed in the presence of the polarizable continuum. Second, gas-phase calculations (with no PCM model) employing up to 5 explicit water solvent molecules around the proton-bound dimers were used to investigate specific adenine-solvent interactions.

3. Results and Discussion

3.1. Computed Structures and Thermochemistry of Adenine Proton-Bound Dimers. The four lowest-energy structures of the adenine proton-bound dimer are shown in parts A−D in Figure 1. These structures were first presented by Hud and Morton.[45] They are planar and best described as N3 or N1 protonated N9H adenine tautomers interacting with the N7H neutral tautomer of adenine. At the B3LYP level, they lie some

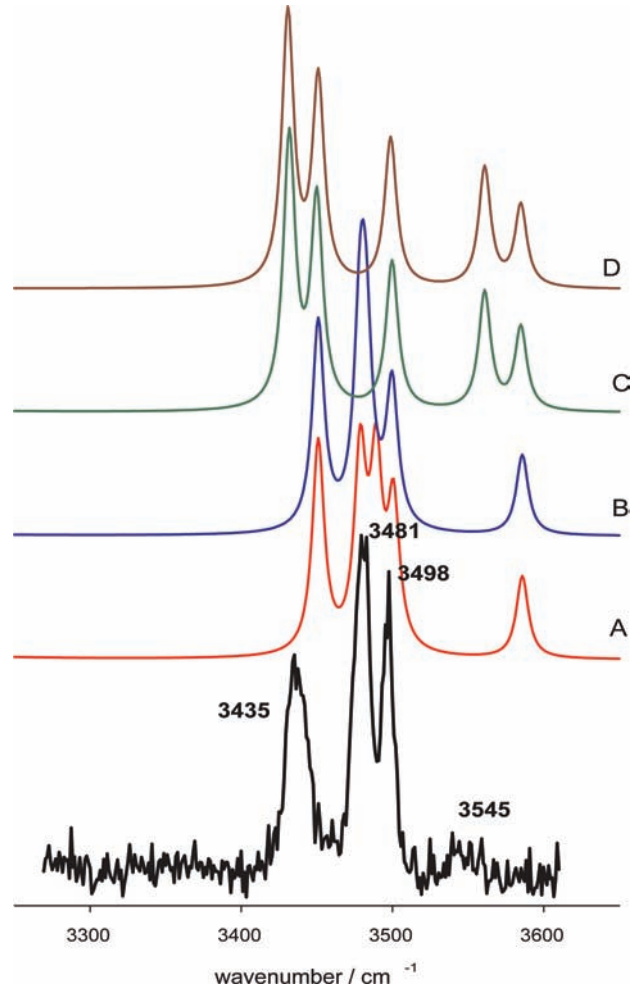

Figure 3. Comparison of the experimental IRMPD spectrum of the adenine proton-bound dimers with the B3LYP/6-31+G(d,p) predicted IR spectra for structures A−D (structures in Figure 1).

20 kJ mol^{-1} lower in enthalpy than the proton-bound dimers stemming from the N9H tautomers (E−J in Figure 2).[45]

To begin, we validate the B2P3LYP functional for these systems by comparing the predicted binding energies for the proton-bound adenine dimer with the experimental value of ΔH(500 K) = 127 ± 4 kJ mol^{-1} measured by Mautner using high-pressure mass spectrometry experiments.[27] The binding energies are computed relative to the adenine N9H tautomer and the N1-protonated adenine N9H tautomer.[58] These results are summarized in Table 1. As has been noted earlier,[45] B3LYP underestimates the interaction energy for the proton-bound dimer by about 20 kJ mol^{-1}. In contrast, three of the B2P3LYP-predicted isomer interaction energies lie within the experimental uncertainty, and the fourth lies only 1 kJ mol^{-1} outside of that range. Both B3LYP and B2P3LYP suggest that isomer A is the most stable, but the small energy differences between the four structures prevent a definitive prediction of the most stable gas-phase structure. Overall, these results suggest that the B2P3LYP functional performs better than B3LYP for this system. In the remaining sections, we will use B2P3LYP to confirm the B3LYP predictions.

The relative energies of the four lowest-energy proton-bound dimers computed here and energies for these and other structures published previously[9] are summarized in Table 2. MP2/6-311++G(2d,p)//B3LYP/6-31+G** energies agree with the relative energetic ordering from Hud and Morton[45] and Liu et al.[9] The relative energies of these species suggest that the

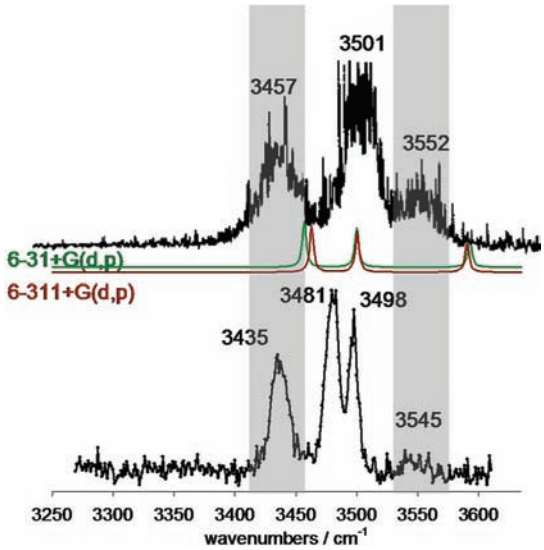

Figure 4. Comparison of the experimental IRMPD spectrum of the adenine proton-bound dimer with the gas-phase spectrum of neutral adenine. Also shown are predicted spectra for the N9H tautomer of neutral adenine.

higher energy structures, E−L, are unlikely to be present in significant quantities experimentally.

3.2. IRMPD Spectroscopy. Upon absorption of infrared radiation from the OPO laser, the adenine proton-bound dimer (*m*/*z* 271) dissociates to produce protonated adenine (*m*/*z* 136). No other products were observed.

The IRMPD efficiency spectrum in the 3250−3650 cm^{-1} region is shown as the black trace at the bottom of Figure 3. The computed spectra in Figure 3 will be discussed below. There are three strong features at 3435, 3481, and 3498 cm^{-1} as well as a much weaker absorption at 3545 cm^{-1}. The two flanking bands can be assigned to the NH_2 symmetric stretching (3435 cm^{-1}) and the NH_2 antisymmetric stretching (3545 cm^{-1}) vibrations based on comparison with experiments conducted on neutral adenine in the gas phase (see Figure 4) and isolated in cryogenic matrices.,[59,60,23] There have been some major differences reported between the experimental and theoretical positions of the NH_2 symmetric and antisymmetric stretching bands for the DNA bases. This is important to justify when comparing the experimental and computed spectra and will be discussed now.

In Figure 4 we compare the experimental IRMPD spectrum of the adenine proton-bound dimer and the IR spectrum of neutral adenine in the gas phase,[60] which agrees very well with the IR spectrum of matrix isolated adenine[23] and the spectrum determined from hole-burning experiments.[59] It is clear from Figure 4 that the NH_2 antisymmetric stretch and symmetric stretches are in very similar positions for the two species. Also in this figure are the spectra predicted by both B3LYP/6-31+G(d,p) and B3LYP/6-311+G(d,p) scaled by 0.957 and 0.9595, respectively. The scaling factor for the B3LYP/6-311+G(d,p) calculations was chosen to match the position of the N−H stretch predicted by the B3LYP/6-31+G(d,p) calculations, the scaling factor of which is a standard one used by our group.[39,44] It can be seen that the observed NH_2 symmetric and antisymmetric stretching bands are significantly to the red of the predicted band positions in both cases. The same "disagreement" in the positions of these particular modes, NH_2 symmetric and antisymmetric stretching, has also been observed with B3LYP/6-31G(d,p) calculations of adenine[2] and cytosine.[12] The reason for the disagreement between experiment and theory is beyond the scope of this paper, but it is important to point out that this disagreement exists and that it must be considered when comparing the experimental and observed spectra of DNA bases and complexes containing an $-NH_2$ group. We are confident in assigning the 3435 and 3545 cm^{-1} features to the symmetric and antisymmetric stretching vibrations of the proton-bound dimer. Finally, very recent anharmonic calculations on neutral adenine predict the asymmetric and symmetric stretching vibrations at 3539 and 3432 cm^{-1}, respectively, in excellent agreement with experimental values.[61] The N−H stretching vibrations predicted by the scaled harmonic calculations and the anharmonic calculations are virtually identical.

TABLE 3: Table of Assignments for Experimental IRMPD Bands for the Adenine Proton-Bound Dimer and Predicted Bands for Structures A−D

		B3LYP/6-31+G(d,p)/cm^{-1}			
observed/cm^{-1}	assignment	A	B	C	D
3435	NH_2 symmetric stretch	3448	3448	3429[a] 3447[b]	3428[a] 3447[b]
3481	A(9)-H stretch	3479	3480		
	free N−H stretch of H-bonded NH_2 group	3490	3483		
3498	A(7)-H stretch	3497	3497	3497	3496
3545	NH_2 antisymmetric stretch	3582	3583	3558[a] 3581[b]	3557[a] 3582[b]

[a] Protonated adenine moiety. [b] Neutral adenine moiety.

The two bands in the experimental proton-bound dimer spectrum observed at 3481 and 3498 cm^{-1} (Figure 3) may be assigned to free N−H stretching bands based on their positions. Throughout this paper "free N−H" denotes an N−H group that is not involved in hydrogen bonding, which would strongly red-shift the N−H stretch out of the observable IR region. The band observed at 3501 cm^{-1} (Figure 4) for neutral adenine is the N9−H stretch. In the proton-bound dimer the band at 3498 cm^{-1} is in agreement with the theoretically predicted N7−H stretch of the neutral adenine moiety, for all four lowest energy structures, A−D (see Figure 1). In the proton-bound dimer spectrum the band centered at 3481 cm^{-1} is not observed in the neutral adenine spectrum and is not predicted for structures C and D. In structures C and D as well as neutral adenine, there is only one free N−H moiety. However, in proton-bound dimers A and B there are two free N−H groups. This closely resembles the positions of the predicted absorptions for the N9−H stretch of the protonated adenine moiety for proton-bound dimer structures A and B (see Table 3). At almost the same frequency is the free N−H stretch of the amino group involved in hydrogen bonding. This feature observed in the experimental spectrum does not rule out structures C and D from being present in the gas phase, but it does show that structures A and B are present and perhaps even dominant species based upon the relative intensities.

Also in Figure 3 are the B3LYP/6-31+G(d,p)-predicted IR spectra for the four lowest energy proton-bound dimers, A−D. As discussed above, C and D alone cannot account for the experimental spectrum since the second N−H stretches at 3481 cm^{-1} is not predicted for them. Either of the structures A or B could account for the experimental spectrum since all of the features are accounted for in the predicted spectra. According to the predicted gas-phase thermochemistries, all four isomers are essentially isoenergetic, at least to within the computational error bars.

TABLE 4: Relative Enthalpies[a] (Relative Free Energies in Parentheses) of Solvated and Unsolvated Adenine Proton-Bound Dimers A, B, C, and D

	unsolvated	PCM B3LYP/6-31+G**	5 waters	5 waters + PCM
A	0.0 (0.0)	0.0 (0.0)	0.0 (0.0)	0.0 (0.0)
B	3.1 (1.9)	−0.1 (−0.1)	3.5 (4.2)	−0.2 (0.6)
C	0.5 (1.1)	9.5 (10.4)	21.8 (20.7)	10.6 (11.2)
D	2.2 (2.3)	9.3 (10.5)	22.8 (22.9)	10.2 (11.7)

[a] Unless otherwise stated, all energies are B2P3LYP/cc-pVTZ//B3LYP/6-31+G(d,p), 298 K values.

However, if structures C and D are prevalent contributors to the experimental spectrum, the predicted spectra suggest that there would be two each of the NH_2 symmetric and antisymmetric stretching bands or that the experimental bands might be significantly broader than observed. While it is difficult to ascertain whether the weak band at 3545 cm^{-1} is split, the strong band centered at 3435 cm^{-1} does not resemble two bands nor is it significantly broadened. Calculations predict a difference of about 20 cm^{-1} between the two NH_2 symmetric stretching vibrations of C and D (see Table 3). The two bands at 3481 and 3498 cm^{-1} in the Experimental spectrum are well-resolved, so we would expect, if C and D are present, that there would be two bands around 3435 cm^{-1}.

3.3. Aqueous Solvation Effects on Dimer Stabilities. Working under the hypothesis that structures A and B are mainly responsible for the experimental infrared spectrum of the adenine proton-bound dimer, an explanation for why structures C and D can be ruled out, even though the gas-phase thermochemistries predict virtually equal amounts of all four (Table 4), is needed. Because these proton-bound dimers are initially formed in solution before being electrosprayed and desolvated, we explore the effects of solvation on the relative stabilities of the different isomers. Solvent effects remain challenging to address quantum mechanically, so two different approaches are used to investigate them. As we will demonstrate, both solvent models predict qualitatively similar results, suggesting that the models are capturing important physical effects.

First, a polarizable continuum model is used to approximate bulk solvation effects. The geometries of all four structures were therefore reoptimized using the PCM with water (dielectric = 78.39) as the solvent at the B3LYP/6-31+G(d,p) level. Frequency calculations were also performed in the presence of the PCM. The thermochemical results of the PCM calculation are shown in Table 4. According to the PCM calculations, water preferentially stabilizes structures A and B significantly with respect to C and D.

To look at specific localized solvent interaction, the explicit microsolvation using a handful of water molecules was examined. By use of five water molecules, all hydrogen-bond donors and acceptors on the proton-bound dimers can be saturated with water molecules. These structures, which could reasonably correspond to the innermost solvent coordination layer in bulk water, are presented in Figure 5, and their relative B2P3LYP/cc-pVTZ energies are listed in Table 4. In contrast to the gas-phase results, and in good agreement with the PCM ones, the A/B microsolvated structures are substantially more stable than the C/D ones. Similarly, calculations employing both the explicit solvent molecules and the PCM model provide energies consistent with the explicit-only and PCM calculations (Table 4). Simple equilibrium constant calculations based on either the microsolvated or PCM relative free energies suggest that mixtures of isomers A−D in solution will contain less than 1% each of C and D at 298 K. The ratio of A to B depends on the exact free energies used, but it ranges from almost a 50:50 mixture (PCM) to 84% A (5-water microsolvated). These results

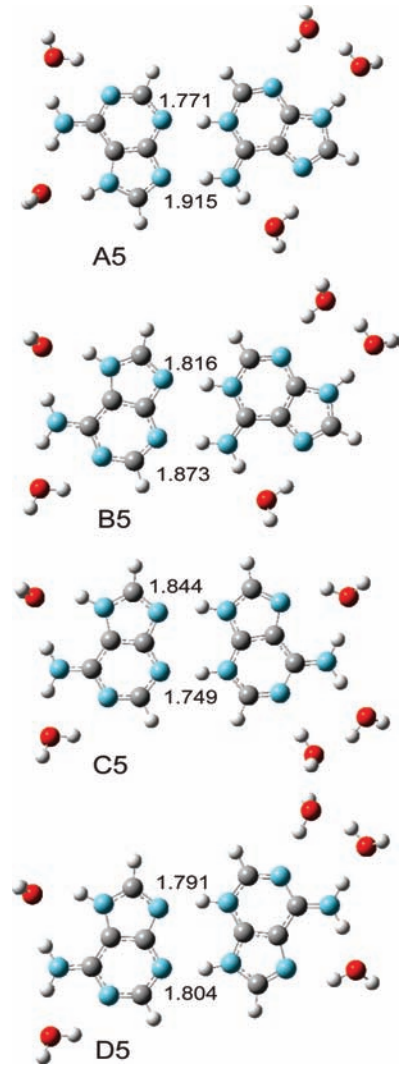

Figure 5. B3LYP/6-31+G(d,p) structures of the four lowest-energy adenine proton-bound dimers microsolvated with five water molecules.

TABLE 5: 298 K Relative Enthalpies (and Free Energies) for Singly Solvated Adenine Proton-Bound Dimers (See Figure 6 for Structures)

structure	relative *H* (*G*)[a] B2P3LYP/cc-pVTZ//B3LYP/6-31+G**
A1i	0.0 (0.0)
A1ii	12.4 (8.3)
A1iii	17.0 (4.5)
A1iv	23.8 (20.8)
B1i	3.0 (3.1)
B1ii	15.7 (13.4)
B1iii	21.5 (10.5)
B1iv	26.3 (24.2)
C1i	−0.3 (−0.8)
C1ii	14.2 (11.9)
C1iii	24.4 (21.2)
C1iv	28.6 (14.3)
D1i	1.4 (0.9)
D1ii	15.0 (12.9)
D1iii	25.8 (22.9)
D1iv	30.3 (15.9)

[a] 298 K.

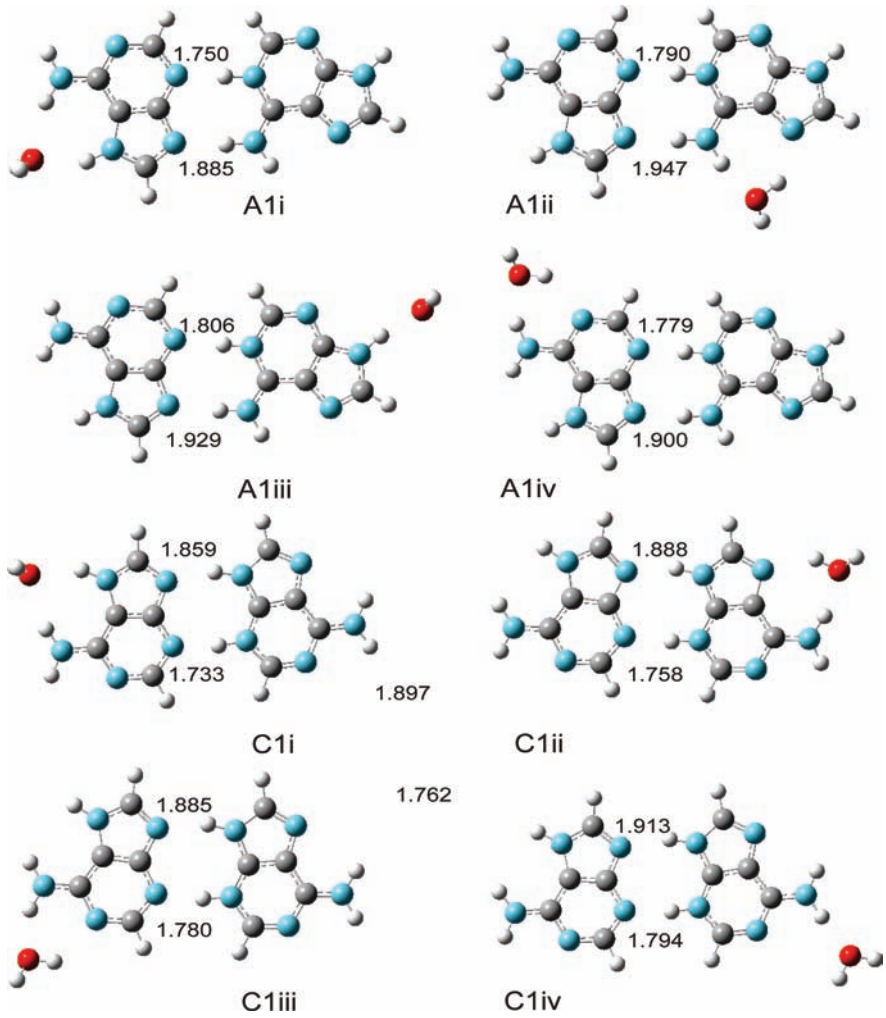

Figure 6. The four B3LYP/6-31+G(d,p) singly microsolvated structures each for A and C. Microsolvated structures for B and D are in Figure S1 of Supporting Information.

are consistent with the interpretation of the IRMPD spectrum discussed above.

Examining these results in more detail, Table 5 lists the relative stabilities of the singly solvated A and C dimer structures presented in Figure 6. (Solvated structures for B and D are in Figure S1 of Supporting Information.) The four single water molecule solvation sites are the most acidic available sites on each of the proton-bound dimers. Each solvation site donates a proton from the adenine to the water, and two of these sites also have an adjacent proton-acceptor site, which accepts a hydrogen bond from the water molecule. The key difference between the A/B and the C/D dimers is the orientation of the NH_2 group on the right adenine molecule. In A/B, this group is directly involved in the proton-bound dimer formation, while in C/D it is completely accessible to the solvent. A water−adenine hydrogen bond at this site on the side opposite the 5-membered ring is the least favored position, as is clear from the relative energies of structures A1iv, C1iii, and C1iv (23.8, 24.4, and 28.6 kJ mol^{-1}, respectively). Because C/D have two such solvent-accessible sites, they are stabilized less in water than are the A/B proton-bound dimers.

Neither the PCM model nor the explicitly microsolvated model truly describes the bulk water solvation effects. However, both models provide the same results: structures C and D are significantly less stable in water than are A and B. Because the dimers are formed in solution prior to electrospray, we propose that the relative stability of these dimers in solution determines which isomers are observed in the IRMPD spectrum. This hypothesis assumes that the dimers A and/or B do not isomerize to C and/or D in the gas phase. This assumption seems reasonable, given that the binding energies of these proton-bound dimers are approximately 120−130 kJ/mol and that substantial disruption of the hydrogen bonding and tautomerization would be required, resulting in a significant energy barrier for isomerization of A or B to C or D. In other words, isomerization seems unlikely on the time scale of the electrospray/desolvation process. This hypothesis is consistent with the apparent absence of strong signals for isomers C and D in the spectra. In contrast, the gas-phase energies which find all four structures nearly degenerate, cannot explain this observation.

3.4. Comparison of IRMPD Spectrum With Higher-Energy Isomers. In Figure 7 the IRMPD spectrum is compared to the computed spectra for structures E−L. Structures I and J have multiple strong bands in the lower-energy portion of the spectrum and therefore can be ruled out on spectroscopic grounds. However, structures E, F, G H, K, and L cannot be equivocally ruled out based solely by comparing of the experimental and computed spectra. These structures alone cannot account for the spectrum, but the absence of predicted bands does not rule them out. Structures E through L can, though, be ruled out based on their computed energies. Even

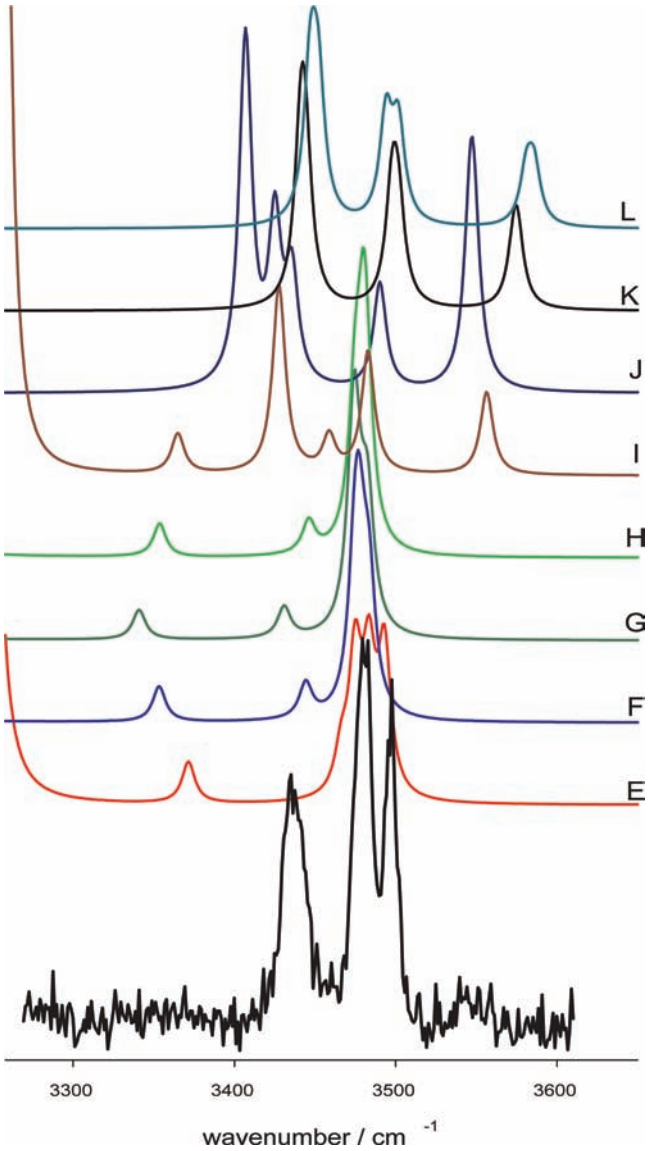

Figure 7. Comparison of the experimental IRMPD spectrum of the adenine proton-bound dimers with the B3LYP/6-31+G(d,p) predicted IR spectra for structures E−L (structures in Figure 2).

PCM calculations with these structures do not lower their energies with respect to A and B.

Conclusions

Gas-phase calculations predict four isoenergetic isomers of the proton-bound adenine dimer. In contrast the IRMPD spectrum of electrosprayed adenine proton-bound dimers with the predicted IR spectra reveal that only two of the isomers are present. PCM model calculations and microsolvation calculations with 5 explicit water molecules qualitatively agree that solvation significantly stabilized two of the four lowest energy isomers. These two solvent-stabilized isomers are consistent with the interpretation of the IRMPD spectrum. This work demonstrates that in some cases, using gas-phase calculations to predict the structures of ions born in solution and transferred to the gas-phase via electrospray ionization can give misleading results.

Acknowledgment. T.D.F. wishes to thank CFI and NSERC for generous funding. ACE-Net is acknowledged for valuable computational resources. E.A.L.G. thanks NSERC for funding in the form of a CGS-D. The scientific staff at CLIO are gratefully acknowledged. G.B. wold like to thank the University of California, Riverside, for financial support. Helpful discussions with and a careful reading of our manuscript by Tom Morton are gratefully acknowledged.

Supporting Information Available: Images of the solvated structures for B and D. This information is available free of charge via the Internet at http://pubs.acs.org.

References and Notes

(1) Seeman, N. C. *Nature* **2003**, *421*, 427.
(2) Mao, C.; LaBean, T.; Reif, J. H.; Seeman, N. C. *Nature* **2000**, *407*, 493.
(3) Cheng, Y. T.; Wang, Z. M.; Liao, C. S.; Yan, C. H. *New. J. Chem.* **2002**, *26*, 1360.
(4) Gu, J.; Leszezynski, J. *J. Phys. Chem. A* **1999**, *103*, 2744.
(5) Sukhanov, O. S.; Shishkin, O. V.; Gorb, L.; Podolyan, Y.; Leszczynski, J. *J. Phys. Chem. B* **2003**, *107*, 2846.
(6) Del Bene, J. E. *J. Phys. Chem.* **1983**, *87*, 367.
(7) Chandra, A. K.; Nguyen, M. T.; Uchimaru, T.; Zeegers-Huyskens, T. *J. Phys. Chem. A* **1999**, *103*, 8853.
(8) Mennucci, B.; Toniolo, A.; Tomasi, J. *J. Phys. Chem. A* **2001**, *105*, 4749.
(9) Liu, B. P.; Ding, Y. J.; Yuan, X. A. *THEOCHEM* **2008**, *848*, 47.
(10) Park, H. S.; Nam, S. H.; Song, J. K.; Park, S. M.; Ryu, S. *J. Phys. Chem. A* **2008**, *112*, 9023.
(11) Delchev, V. B.; Shterev, I. G.; Mikosch, H.; Kochev, N. T. *J. Mol. Model* **2007**, *13*, 1001.
(12) Wang, F.; Downton, M. T.; Kidwani, N. *J. Theor. Comput. Chem.* **2005**, *4*, 247.
(13) Zierkiewicz, W.; Komorowski, L.; Michalska, D.; Cerny, J.; Hobza, P. *J. Phys. Chem. B.* **2008**, *112*, 16734.
(14) Herrera, B.; Toro-Labbe, A. *J. Phys. Chem. A* **2007**, *111*, 5921.
(15) Florian, J.; Leszczynski, J. *J. Am. Chem. Soc.* **1996**, *118*, 3017.
(16) Lowdin, P. O. *Adv. Quantum Chem.* **1965**, *2*, 213.
(17) Topal, M. D.; Fresco, J. R. *Nature* **1976**, *263*, 285.
(18) Hanus, M.; Kabalac, M.; Rejnek, J.; Ryjacek, F.; Hobza, P. *J. Phys. Chem. B* **2004**, *108*, 2087.
(19) Guerra, C. F.; Bickelhaupt, F.; Saha, S.; Wang, F. *J. Phys. Chem. A* **2006**, *110*, 4012.
(20) Turecek, F.; Chen, X. *J. Am. Soc. Mass Spectrom.* **2005**, *16*, 1713.
(21) Bell, R. L. *The tunnel effect in Chemistry*; Chapman and Hall: New York, 1980.
(22) Curtiss, L. A.; Drapcho, D. L.; Pople, Y. A. *Chem. Phys. Lett.* **1984**, *103*, 437.
(23) Nowak, M. J.; Lapinski, L.; Kwiatkowski, J. S.; Leszezynski, J. *J. Phys. Chem.* **1996**, *100*, 3527.
(24) Bonaccorsi, B.; Pullman, A.; Scrocco, E.; Tomasi, J. *Theor. Chim. Acta* **1972**, *24*, 51.
(25) Russo, N.; Toscana, M.; Grand, A.; Jolibois, F. *J. Comput. Chem.* **1998**, *19*, 989.
(26) Podolyan, Y.; Gorb, L.; Leszczynski, J. *J. Phys. Chem. A* **2000**, *104*, 7346.
(27) Meot-Ner, M. *J. Am. Chem. Soc.* **1979**, *101*, 2396.
(28) Wolken, J. K.; Turecek, F. *J. Am. Soc. Mass Spectrom.* **2000**, *11*, 1065.
(29) Greco, F.; Liguori, A.; Sindona, G.; Uccelle, N. *J. Am. Chem. Soc.* **1990**, *112*, 9092.
(30) Kumar, G. S.; Das, S.; Bhadra, K.; Maiti, M. *Bioorg. Med. Chem.* **2003**, *11*, 4861.
(31) Chen, F. M. *Biochemistry* **1984**, *23*, 6159.
(32) Volker, J.; Klump, H. H. *Biochemistry* **1994**, *33*, 13502.
(33) Wilson, W. D.; Tanious, F. A.; Mizan, S.; Yao, S.; Kiselyov, A. S.; Zon, G.; Strekowski, L. *Biochemistry* **1993**, *32*, 10614.
(34) Cooney, M.; Czernusszewicz, G.; Postel, E. H.; Flint, S. J.; Hogan, M. E. *Science* **1988**, *241*, 456.
(35) Marian, C.; Nolting, D.; Weinkauf, R. *Phys. Chem. Chem. Phys.* **2005**, *7*, 3306.
(36) Fridgen, T. D. *Mass Spectrom. Rev.* **2009**, *28*, 586.
(37) Polfer, N. C.; Oomens, J. *Mass Spectrom. Rev.* **2009**, *28*, 468.
(38) Eyler, J. R. *Mass Spectrom. Rev.* **2009**, *28*, 448.
(39) Atkins, C. G.; Rajabi, K.; Gillis, E. A. L.; Fridgen, T. D. *J. Phys. Chem. A* **2008**, *112*, 10220.
(40) Rajabi, K.; Fridgen, T. D. *J. Phys. Chem. A* **2008**, *112*, 23.
(41) Yoon, S. H.; Chamot-Rooke, J.; Perkins, B.; Hilderbrand, A. E.; Poutsma, J. C.; Wysocki, V. H. *J. Am. Chem. Soc.* **2008**, *130*, 17644.
(42) Salpin, J. Y.; Guillaumont, S.; Tortajada, J.; MacAleese, L.; Lemaire, J.; Maitre, P. *Chem. Phys. Chem.* **2007**, *8*, 2235.

(43) Rajabi, K.; Easterling, M. L.; Fridgen, T. D. *J. Am. Soc. Mass Spectrom.* **2009**, *20*, 411.

(44) Gillis, E. A. L.; Rajabi, K.; Fridgen, T. D. *J. Phys. Chem. A* **2009**, *113*, 824.

(45) Hud, N. V.; Morton, T. H. *J. Phys. Chem. A* **2007**, *111*, 3369.

(46) Bakker, J. M.; Besson, T.; Lemaire, J.; Scuderi, D.; Maitre, P. *J. Phys. Chem. A* **2007**, *111*, 13415.

(47) Frisch, M. J.; Trucks, G. W.; Schlegel, H. B.; Scuseria, G. E.; Robb, M. A.; Cheeseman, J. R.; Montgomery, J. A., Jr.; Vreven, T.; Kudin, K. N.; Burant, J. C.; Millam, J. M.; Iyengar, S. S.; Tomasi, J.; Barone, V.; Mennucci, B.; Cossi, M.; Scalmani, G.; Rega, N.; Petersson, G. A.; Nakatsuji, H.; Hada, M.; Ehara, M.; Toyota, K.; Fukuda, R.; Hasegawa, J.; Ishida, M.; Nakajima, T.; Honda, Y.; Kitao, O.; Nakai, H.; Klene, M.; Li, X.; Knox, J. E.; Hratchian, H. P.; Cross, J. B.; Bakken, V.; Adamo, C.; Jaramillo, J.; Gomperts, R.; Stratmann, R. E.; Yazyev, O.; Austin, A. J.; Cammi, R.; Pomelli, C.; Ochterski, J. W.; Ayala, P. Y.; Morokuma, K.; Voth, G. A.; Salvador, P.; Dannenberg, J. J.; Zakrzewski, V. G.; Dapprich, S.; Daniels, A. D.; Strain, M. C.; Farkas, O.; Malick, D. K.; Rabuck, A. D.; Raghavachari, K.; Foresman, J. B.; Ortiz, J. V.; Cui, Q.; Baboul, A. G.; Clifford, S.; Cioslowski, J.; Stefanov, B. B.; Liu, G.; Liashenko, A.; Piskorz, P.; Komaromi, I.; Martin, R. L.; Fox, D. J.; Keith, T.; Al-Laham, M. A.; Peng, C. Y.; Nanayakkara, A.; Challacombe, M.; Gill, P. M. W.; Johnson, B.; Chen, W.; Wong, M. W.; Gonzalez, C.; Pople, J. A. *Gaussian 03*, revision B.04; Gaussian, Inc.: Wallingford, CT, 2004.

(48) Benighaus, T.; Distasio, R. A., Jr.; Lochan, R. C.; Chai, J.; Head-Gordon, M. *J. Phys. Chem. A* **2008**, *112*, 2702.

(49) Dunning, T. H. *J. Chem. Phys.* **1989**, *90*, 1007.

(50) Kristyan, S.; Pulay, P. *Chem. Phys. Lett.* **1994**, *229*, 175.

(51) (a) Grimme, S. *J. Chem. Phys.* **2006**, *124*, 034108. (b) Schwabe, T.; Grimme, S. *Phys. Chem. Chem. Phys.* **2007**, *9*, 3397.

(52) Boys, S. F.; Bernardi, F. *Mol. Phys.* **1970**, *19*, 553–566.

(53) Shao, Y.; Molnar, L. F.; Jung, Y.; Kussmann, J.; Ochsenfeld, C.; Brown, S. T.; Gilbert, A. T. B.; Slipchenko, L. V.; Levchenko, S. V.; O'Neill, D. P.; DiStasio, Jr, R. A.; Lochan, R. C.; Wang, T.; Beran, G. J. O.; Besley, N. A.; Herbert, J. M.; Lin, C. Y.; Van Voorhis, T.; Chien, S. H.; Sodt, A.; Steele, R. P.; Rassolov, V. A.; Maslen, P. E.; Korambath, P. P.; Adamson, R. D.; Austin, B.; Baker, J.; Byrd, E. F. C.; Dachsel, H.; Doerksen, R. J.; Dreuw, A.; Dunietz, B. D.; Dutoi, A. D.; Furlani, T. R.; Gwaltney, S. R.; Heyden, A.; Hirata, S.; Hsu, C.-P.; Kedziora, G.; Khalliulin, R. Z.; Klunzinger, P.; Lee, A. M.; Lee, M. S.; Liang, W. Z.; Lotan, I.; Nair, N.; Peters, B.; Proynov, E. I.; Pieniazek, P. A.; Rhee, Y. M.; Ritchie, J.; Rosta, E.; Sherrill, C. D.; Simmonett, A. C.; Subotnik, J. E.; Woodcock, III, H. L.; Zhang, W.; Bell, A. T.; Chakraborty, A. K.; Chipman, D. M.; Keil, F. J.; Warshel, A.; Hehre, W. J.; Schaefer, H. F., III; Kong, J.; Krylov, A. I.; Gill, P. M. W.; Head-Gordon, M. *Phys. Chem. Chem. Phys.* **2006**, *8*, 3172–3191.

(54) (a) Dunlap, B. I. *J. Chem. Phys.* **1983**, *78*, 3140. (b) Feyereisen, M.; Fitzgerald, G.; Komornicki, A. *Chem. Phys. Lett.* **1993**, *208*, 359. (c) Eichkorn, K.; Treutler, O.; Öhm, H.; Häser, M.; Ahlrichs, R. *Chem. Phys. Lett.* **1995**, *240*, 283.

(55) Weigend, F.; Köhn, A.; Hättig, C. *J. Chem. Phys.* **2002**, *116*, 3175.

(56) Steele, R. P.; Distasio, R. A., Jr.; Shao, Y.; Kong, J.; Head-Gordon, M. *J. Chem. Phys.* **2006**, *125*, 074108.

(57) Cossi, M.; Rega, N.; Scalmani, G.; Barone, V. *J. Comput. Chem.* **2003**, *24*, 669.

(58) The stability of the N3-protonated adenine N7H tautomer is computed to be nearly the same as the N1-protonated adenine N9H tautomer, as they differ by only a fraction of a kJ/mol. Which species is more stable depends on exactly which functional and basis set is used, but for B2P3LYP/cc-pVTZ, the N1H/9H species is 0.4 kJ/mol more stable. These relative stabilities of the two tautomers agrees well with the experimental results from ref 35.

(59) Plutzer, C.; Kleinermanns, K. *Phys. Chem. Chem. Phys.* **2002**, *4*, 4877.

(60) Colarusso, P.; Zhang, K.; Guo, B.; Bernath, P. *Chem. Phys. Lett.* **1997**, *269*, 39.

(61) Zierkiewicz, W.; Komorowski, L.; Michalaska, D.; Cerny, J.; Hobza, P. *J. Phys. Chem. B.* **2008**, *112*, 16734.

JP9033062